Tutors
Dr. Francesc Viñes Solana
Departament de Ciència de Materials i Química Física
Dr. Pablo Gamallo Belmonte
Departament de Ciència de Materials i Química Física

Grau de Química

Treball Final de Grau

Modification of 2D Graphene Membranes for Biogas Enrichment Using Machine-Learning Force Fields
Modificació de membranes 2D de grazins per l'enriquiment de biogàs amb camps de forces d'aprenentatge automàtic

Biel Garrrote Ferré

Juny de 2025

Universitat de Barcelona
B:KC Barcelona Knowledge Campus
Campus d'Excel·lència Internacional

Fill, tu pots.

La meva mare

No es que sea muy listo, es que me quedo con los problemas más tiempo.

Albert Einstein

En primer lloc, voldria agrair als meus dos tutors, en Fransis i en Pablo, pel seu esforç incansable des del primer dia que va començar aquesta aventura, ara fa uns mesos. Gràcies als dos per haver-me ensenyat una part de la química en què no m'havia fixat gaire i de la qual me'n porto un molt bon record. En segon lloc, voldria agrair a tots els amics que han estat amb mi durant aquests anys de carrera, i que han fet d'aquesta experiència, una experiència inoblidable. Per últim, vull agrair a la meva família per tots els ànims, el recolzament, els consells, els esforços i l'amor que m'han brindat al llarg d'aquests quatre anys. Us estimo.

REPORT

IDENTIFICATION AND REFLECTION ON THE SUSTAINABLE DEVELOPMENT GOALS *(SDG)*

This final degree project is based on the modification and use of materials such as grazynes in biogas purification, particularly in studying the influence of the halogen substitution in the nanopores. These materials are possible candidates as membranes for gas separation of CO_2 and CH_4. This work is highly relevant with respect to a number of the United Nations Sustainable Development Goals *(SDGs)* including **SDG 7 (Affordable and Clean Energy)**, **SDG 9 (Industry, Innovation and Infrastructure)**, and **SDG 13 (Climate Action)**.

SDG 7 is all about ensuring universal access to affordable, reliable and modern energy services. Biogas energy is the renewable energy that can help to achieve that, being a renewable option to the classic fossil fuels. Studies of selective CO_2 and CH_4 separation for pure biogas will increase the combustion efficiency, decrease the emission of greenhouses gases, and increase the overall energy yield.

SDG 9 attempts to develop resilient infrastructure, promote inclusive and sustainable industrialization, and support innovation. Two-dimensional materials such as halogen-modified grazynes represent a significant technological advancement in gas purification. Developing new materials with high selectivity and separation efficiency opens the door to new industrial applications, to boost technological competitiveness, and encourages the adoption of more sustainable alternatives.

SDG 13 demands immediate measures to mitigate climate changes and its effects. The reduction of greenhouse gas emissions, specifically CO_2 and CH_4, is extremely important in addressing the global warming problem. Research of technologies which facilitate the handling and minimisation of these emissions, is crucial to reach the international climate goals.

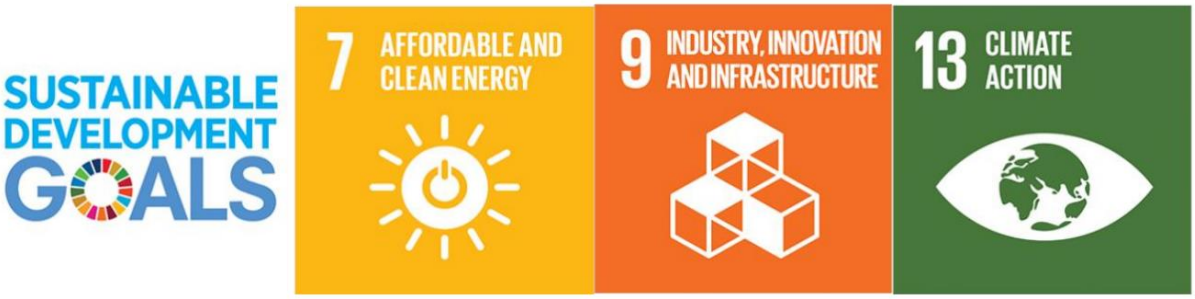

CONTENTS

1. SUMMARY

The present project explores the use of grazynes, two-dimensional (2D) carbon allotropes nanoengineered with nanopores, as an innovative solution for separating CO_2 and CH_4 in biogas. This is achieved by performing substitutions of the hydrogen atoms originally located at the pore sites with different halogens (F, Cl, and Br). The system is assessed through theoretical simulations using Density Functional Theory (*DFT*), employing the Perdew–Burke–Ernzerhof (*PBE*) exchange-correlation functional, and including dispersive interactions *via* the Grimme D3 method (*PBE-D3*).

The analysis focused on the diffusion of CO_2 and CH_4 through the pores of various halogenated grazynes. Adsorption energies and penetration energy barriers for both molecules were calculated, revealing that CO_2 exhibits low adsorption and diffusion barriers, while CH_4 shows also low adsorption energies, but with significantly higher barriers. This implies that fluorinated grazynes are promising candidates for biogas upgrading. However, chlorine and bromine substitutions increase the atomic radius at the pore, reducing permeability and making these materials unsuitable for gas separation. Subsequently, diffusion rate constants were computed using Transition State Theory (*TST*), confirming that only fluorinated grazynes present large enough rate constants (*k*), indicating effective gas permeation, while chlorinated and brominated grazynes yield values close to zero, highlighting their poor performance as separation membranes. Thus, CO_2 could be largely selectively separated when using defective [1],[2]{2}-tetrafluorograzyne, specially when goes through various penetration cycles.

The [1],[2]{2}-fluorograzyne and [1],[2]{2}-o-difluorograzyne were subjected to further study *via* Molecular Dynamics (*MD*) simulations using Machine-Learning Force Fields (*ML-FF*). Although the force field exhibited low training errors, the MD trajectories displayed chemically unrealistic behaviour, *e.g.* bent CO_2, implying that the model had not been exposed to a sufficiently diverse training set. Thermodynamic plots showed a sudden increase in temperature and energy during the simulation, which confirms that the system adopted unrealistic atomic configurations. Therefore, the force field must be trained with more data to ensure accurate and reliable MD-MLFF results.

Keywords: Density Functional Theory, Grazynes, Machine-Learning, Molecular Dynamics, Biogas Upgrading.

2. RESUM

El present projecte de recerca explora l'ús dels grazins, al·lòtrops de carboni bidimensionals (2D) amb nanopors, com una solució innovadora per a la separació de CO_2 i CH_4 en el biogàs. Això s'aconsegueix mitjançant la substitució dels àtoms d'hidrogen que originalment es troben als llocs del porus per diferents halògens (F, Cl i Br). El sistema s'avalua a través de simulacions teòriques usant la Teoria del Funcional de la Densitat *(DFT*), emprant el funcional d'intercanvi-correlació Perdew–Burke–Ernzerhof (*PBE*) i incloent interaccions dispersives mitjançant el mètode de Grimme D3 (*PBE-D3*).

L'anàlisi es va centrar en la difusió de CO_2 i CH_4 a través de les porus de diversos grazins halogenats. Es van calcular les energies d'adsorció i les barreres d'energia per a la penetració de tots dos gasos, revelant que el CO_2 presenta baixes barreres d'adsorció i difusió, mentre que el CH_4 mostra barreres molt més altes. Això implica que els grazins fluorats són candidats prometedors per a la millora del biogàs. No obstant això, les substitucions amb clor i brom augmenten el radi atòmic a la porus, reduint la permeabilitat i fent que aquests materials siguin inadequats per a la separació dels gasos. Posteriorment, es van calcular les constants de velocitat de difusió mitjançant la Teoria de l'Estat de Transició, confirmant que només els grazins fluorats presenten constants de velocitat (k) positives, indicant una permeació efectiva del gas, mentre que els grazins clorats i bromats obtenen valors propers a zero, cosa que destaca el seu pobre rendiment com a membranes de separació. Així, el CO_2 es podria separar amb un 100 % de selectivitat mitjançant l'ús del grazí [1],[2]{2}-tetrafluorograzí.

Els [1],[2]{2}-fluorograzí i [1],[2]{2}-o-difluorograzí van ser sotmesos a un estudi posterior mitjançant simulacions de Dinàmica Molecular (*MD*) amb Camps de Forces d'Aprenentatge Automàtic (*ML-FF*). Tot i que el camp de forces presentava baixos errors d'entrenament, les trajectòries MD mostraven un comportament químicament irreal, per exemple, CO_2 doblegat, cosa que implica que el model no havia estat exposat a un conjunt d'entrenament prou divers. Els gràfics termodinàmics mostraven un augment sobtat de la temperatura i l'energia durant la simulació, confirmant que el sistema adoptava configuracions atòmiques irreals. Per tant, cal entrenar el camp de forces amb més dades per garantir resultats MD-MLFF precisos i fiables.

Paraules clau: Teoria del Funcional de la Densitat, Grazines, Aprenentatge Automàtic, Dinàmica Molecular, Separació de gasos, Biogas.

3. INTRODUCTION

The levels of pollution and emissions in Earth's atmosphere by greenhouses gases, specifically carbon dioxide (CO_2) and methane (CH_4), are continually increasing, representing an important problem for global warming and climate change issues. While CO_2 concentration in the atmosphere exceeds CH_4 by approximately 5%, CH_4 can retain up to 23 times more heat than CO_2, and therefore is important for climate change control.[1] Nowadays, governments and research organizations are dedicating significant resources to develop and improve sustainable energy sources and ways of preventing those emissions. One promising alternative is biogas; an energy source derived from the anaerobic digestion of organic matter.[2] Biogas from organic waste digestion is usually composed of CH_4 (60-70%) mixed with CO_2 (30-40%),[3] which has to be separated in order to increase the commercial value of the fuel. The purity of CO_2 in biogas streams varies between 25% and 50% (v/v), with a purity of 50% to 75% (v/v) of CH_4.[4] For methane to be commercialized as a fuel, a purity above 95% is required.[4]

The chemical resolution of CO_2 from CH_4 is still a big challenge because of the chemical stability and low reactivity of both molecules, making their selective separation a difficult task. Materials for biogas upgrading such as bulk Transition Metal Carbides (*TMCs*),[5] and their two-dimensional (2D) derivates (MXenes),[6] have exhibited promising results in CO_2 capture. However, these materials are subject to poisoning by oxygen adsorption and require expensive regeneration steps. In contrast, 2D carbon-based materials, leaded by graphene nanostructures,[7] and reduced graphene oxides (GO),[8] have emerged as attractive alternatives due to their exceptional mechanical and electronic properties. Graphynes,[9] a family of carbon allotropes composed of *sp*- and sp^2-hybridized carbon atoms, offer a structural versatility that enables precise control over pore size, making them highly suitable for gas separation applications. Various types of membranes also show good results in biogas separation, including polymers,[10] ionic liquids,[11] zeolites,[12] metal-organic frameworks (MOFs),[13] and others. Polymeric and hybrid membranes are the most intensively studied due to their high separation selectivity, good membrane processability, and relatively low cost, where almost all the membranes used in industrial facilities are polymer membranes nowadays.[14]

A novel subclass of graphynes, referred to as grazynes, has been recently developed.[15] Grazynes consist of graphene-like stripes linked by acetylenic bonds, combining the mechanical stability of graphene with the tuneable porosity of graphynes, see Figure 1. This material exhibits distinct structural flexibility, which enables modifications such as lengthening the acetylenic linkages, varying the width of the stripes, and adding acetylenic vacancies to optimize pore dimensions. This degree of tunability makes grazynes as attractive options for membrane-based separations processes, particularly for biogas upgrading. Computational studies using Density Functional Theory (*DFT*) calculations have demonstrated their possibilities.[16]

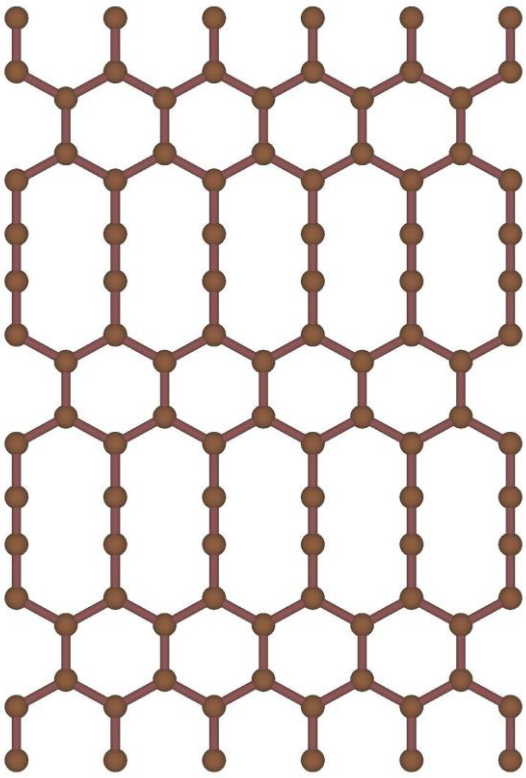

Figure 1: Top view of the [1],[1]-grazyne structure, this is, with the smallest graphene stripe and acetylenic linkage. Brown spheres denote carbon atoms.

Recently, the performance of the grazynes in CO_2/CH_4 separation was studied by tuning the pore structure. In particular, previous investigations focused on acetylenic sites that were removed and capped with hydrogen atoms, which have shown high selectivity for biogas clean-up.[17] The adsorption energy was found to be -0.19 eV for CO_2 and -0.17 eV for CH_4, with diffusion barrier energies below 1 eV for CO_2, and above 1 eV for CH_4. This implies a faster diffusion of CO_2 and an enrichment of CH_4 in the non-permeated gas.

This work is intended to similarly explore the potential of halogenated grazynes as filtration membranes for biogas upgrading, testing the ability to simultaneously maximize CH_4 purity and removal of CO_2 from it. The influence of halogen functionalization on pore-size, diffusion barrier, and overall separation efficiency will be studied carrying out DFT calculations, and also Molecular Dynamics (*MD*) runs, here explorating a new method called Machine-Learning Force-Field *(ML-FF*) generation.

Thus, ML-FF MD is to replace the *Ab Initio* Molecular Dynamics (*AIMD*). While AIMD relies on *e.g.* DFT calculations at each time step, ML-FF MD could automatically interpolate between previously computed *ab initio* data and build force-fields on-the-fly. As a result, the computational cost is significantly reduced, making the simulations much faster. These ML-FF MD will allow us evaluating whether the DFT results are consistent with the actual behaviour of the system when simulating the biogas upgrading mechanism, accounting not only for thermodynamics data, but also for kinetic and dynamic aspects.

4. OBJECTIVES

The main objective of this final degree project is to study the diffusion of CO_2 and CH_4 through two-dimensional (2D) grazyne membranes by determining the diffusion barriers as a function of atomic substitutions within the pore (replacing H capping atom by with halogens such as F, Cl, and Br). To carry out this study, computational calculations will be performed based on DFT, on periodic slab models using the Vienna *Ab Initio* Simulation Package (*VASP*).[18] This package has recently implemented the use of machine learning for the generation of force fields, ML-FF, which allows for a remarkable acceleration of MD simulations.

Other more specific objectives are the following:

- To build and optimize grazynes structures with the different halogen conformations.
- To assess the adsorption energies and the penetration energy barriers for CO_2 and CH_4 with the different grazyne structures.
- To train and refit the ML-FF and assess its accuracy.
- To estimate the diffusion rates constants of the CO_2 and CH_4 molecules.
- To study biogas enrichment by a ML-FF MD and compare the results with DFT.

5. THEORETICAL BACKGROUND

5.1. Schrödinger equation

Schrödinger equation is the basis of Quantum Chemistry. There, the wavefunction Ψ contains all the chemical information, but this wavefunction does not represent any measurable property of the system. However, by applying an operator to it, one can determine the value of a desired property. In this project, the total energy of the system, *E*, is needed to determine whether a suggested grazyne structure is suited for filtering CO_2 or CH_4 molecules. This energy can be determined by solving the time independent Schrödinger equation:

$$\hat{H}\Psi = E\Psi \quad (1),$$

where $\hat{H}$ is the Hamiltonian operator, which includes all kinetic and potential energy contributions, and *E* is the total energy of the system. For polyatomic and polyelectronic molecules, the Hamiltonian can be discomposed into several terms:

$$\hat{H} = \hat{T}_e + \hat{T}_N + \hat{V}_{ee} + \hat{V}_{NN} + \hat{V}_{Ne} \quad (2),$$

including the kinetic energy of electrons ($\hat{T}_e$), the kinetic energy of nuclei ($\hat{T}_N$), the coulombic repulsion between electrons ($\hat{V}_{ee}$), the coulombic repulsion between nuclei ($\hat{V}_{NN}$), and the coulombic attraction between electrons and nuclei ($\hat{V}_{Ne}$). To make things simpler, one usually works under the Born-Oppenheimer (*BO*) approximation. This BO approximation basis in that nuclei are much heavier and move much more slowly than electrons. This allows us considering that the nuclei are practically static from the point of view of electrons, reducing the problem to the electronic Hamiltonian. Thus;

$$\hat{H} = \hat{T}_e + \hat{V}_{ee} + \hat{V}_{Ne} \quad (3).$$

So, the electronic Schrödinger equation becomes:

$$\hat{H}_e\Psi_e = E_e\Psi_e \quad (4).$$

At this point, the mathematical complexity of the system has been reduced. Nevertheless, the exact solution of Eq. 4 can be only obtained for simple systems having only one electron, like hydrogen atoms. For more complex systems, like the 2D materials studied in this project, grazynes, the electronic correlation becomes difficult to estimate, and one needs to use approximate computational methods. Different approximated *ab initio* methods like Hartree-Fock (*HF*), Configuration Interactions (*CI*), or Møller-Plesset perturbational methods, *e.g.* MP2, have been developed, which allow us to get a good approximation of the electronic energy, but at a higher computational cost. To carry out this project we used DFT method, since it is a good compromise between computational cost and accuracy.

5.2. Density functional theory

DFT is one of the most used methods in Quantum Chemistry to study the electronic structure of atoms, molecules, and even solids. It has become a dominant tool simply because the computational costs are relatively low when compared to other wavefunctions methods, without compromising much the accuracy. DFT is based in that the energy of the ground state of a polyelectronic state depends solely, and gets determined by, the electronic density function, ρ(**r**), and therefore, it is not necessary to know the wavefunction to describe the system. The electron density is defined as the electron probabilities all through space by the number of electrons, *N*.

$$\rho(\mathbf{r}) = \mathrm{N}\int \ldots \int |\Psi(\mathrm{x}_1, \mathrm{x}_2, \ldots, \mathrm{x}_\mathrm{N})|^2 \mathrm{dx}_1, \mathrm{dx}_2, \ldots, \mathrm{dx}_\mathrm{N} \quad (5).$$

5.2.1. The Hohenber-Kohn teorems

Although DFT use is nowadays widely extended, it was already developed in 1964 when Hohenberg and Kohn postulated the theoretical basis of the method.[19] Hohenberg and Kohn demonstrated that, for the ground state, there exists a relation between the electronic density and the external potential, $V_{ext}(\mathbf{r})$. This means that the electronic density in the ground state has all the information of the electronic system. In their first theorem, Hohenberg and Kohn showed that the energy can be expressed as an energy functional using the relationship:

$$\mathrm{E}[\rho(\mathbf{r})] = \mathrm{F}[\rho(\mathbf{r})] + \int \rho(\mathbf{r}) v_{\mathrm{Ne}}(\mathbf{r}) \mathrm{d}\mathbf{r} \quad (6),$$

where, $F[\rho(\mathbf{r})]$ represents the universal functional which includes the kinetic energy and the interaction between the electrons, and $v_{Ne}(\mathbf{r})$ is the interaction between the electrons and all the nuclei in a defined position.

The second theorem of Hohenberg and Kohn, HK2, is also called the theorem of the variational principle, and deals with the fact that the energy of the ground state can be obtained variatonally, and that the density that minimizes the total energy is indeed the exact electron density define by the external potential. Any density different from ρ_o, would thus deliver higher energy.

5.2.2. The Kohn-Sham method

The Kohn-Sham (*KS*) method follows the Hohenberg-Kohn theorems, and describes a way to approximate the universal functional.[20] For that, they required as a reference a fictitious system constituted by a homogeneous gas of non-interacting electrons. Within this system, the kinetic energy correspons to the sum of individual kinetic energies and the electronic density to the sum of orbital densities. KS model included the electronic exchange and correlation as well. Thus;

$$\rho(\boldsymbol{r}) = \sum_N^i \mid \phi_i(\boldsymbol{r}) \mid^2 \quad (7),$$

with this, the functional can be descomposed in;

$$E = T_S + E_{ext} + J + E_{xc} \quad (8),$$

where T_s is the kinetic energy of the electrons of the system, E_{ext} corresponds to the attraction between the external potential and the electron density, J represents the coulombic repulsion between electrons, and E_{xc} is the exchange-correlation functional, that corresponds to the difference between the non-interacting electrons system and the real system. The E_{xc} term has no exact definition, but there are different good approximations for estimating it.

5.2.3. Exchange and correlations functionals

As above-mentioned, when using DFT method it is important to know how to approximate the E_{xc} contribution. Nowadays, the exact value of the exchange-correlation (*xc*) functional has not been defined yet. Despite this limitation, numerous approximations have been developed over the years to provide reliable and computationally efficient results. These different strategies for building the *xc* functional are often classified within the framework known as Jacob's Ladder, which ranks the approaches from the most basic to the most sophisticated; see Figure 2.

The simplest and most fundamental method to find xc is the Local Density Approximation (*LDA*), which assumes that the electronic density depends only on spatial coordinates. A more advanced strategy is found in the Generalized Gradient Approximation (*GGA*), which incorporates both the value of the electron density and its gradient. For the purposes of this work, this level of approximation has been adopted, specifically using the Perdew–Burke–Ernzerhof (PBE) *xc* functional, known for its balance between accuracy and computational cost.

Above this level, the meta-GGA functionals appear, which also consider the kinetic energy density by including second derivatives of the density. At the top of the ladder are the hybrid functionals, which mix LDA and/or GGA components with a portion of HF exact exchange, leading to an enhanced precision in many systems, like molecules or semiconductors.

Basic hybrid functionals include only the occupied orbitals, while more complex double hybrid functionals incorporate virtual orbitals as well, and may be considered as the fifth rung of the Jacob's Ladder.

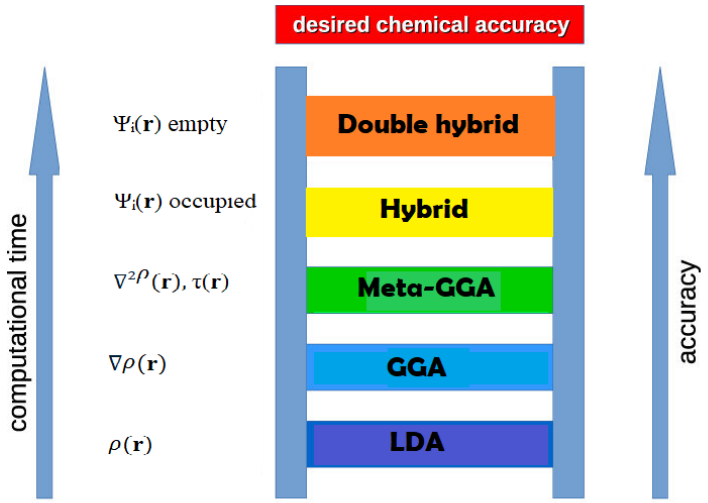

Figure 2: Representation of the different *xc* functionals for DFT within the so-called Jacob's Ladder of improvement.

5.3. 2D carbon allotropes: Grazynes

In recent decades, some 2D allotropes of carbon, such as graphene and graphynes, have been studied in detail, as these compounds have demonstrated remarkable properties in biogas purification.[7,9] Initially, computational calculations were performed to predict the properties and functions of the materials that constitute these allotropes. This project shows a new type of material composed of graphene stripes connected by acetylenic linkages, called grazynes.

Grazynes have its own nomenclature; [n],[m]-grazyne, where the *n* and *m* indicate that the grazynes are built by *n* rings width graphene stripes and with *m* C≡C pairs in the acetylenic linkages.[15] One can see an example of this type of structure in Figure 1, where the [1],[1]-grazyne is represented. When structural defects are introduced into the grazyne, such as pores generated by the removal of acetylenic linkages, they are represented using curly brackets { } in the nomenclature. Figure 3 shows the structure of the [1],[2]{2}-grazyne, an example of a grazyne with structural defects. These defects allow the formation of channels or pores within the structure, which can facilitate the diffusion of small gas molecules such as CO_2 or CH_4 through the material. In this work, we consider such defective structures, which are of great interest for applications like gas separation and molecular sieving.

The grazynes under study show the most promising results in biogas upgrading,[16] due to the possibility of modifying the linkages length and the graphene stripes to get a wide variety of compounds. This together with the possibility of having alternate graphene stripe widths, alternate acetylenic lengths, and with missing acetylenic linkages, opens a vast field of tunability possibilities, as above commented. In this study we use the [1],[2]{2}-grazyne structure in which different halogen substitutions have been done.

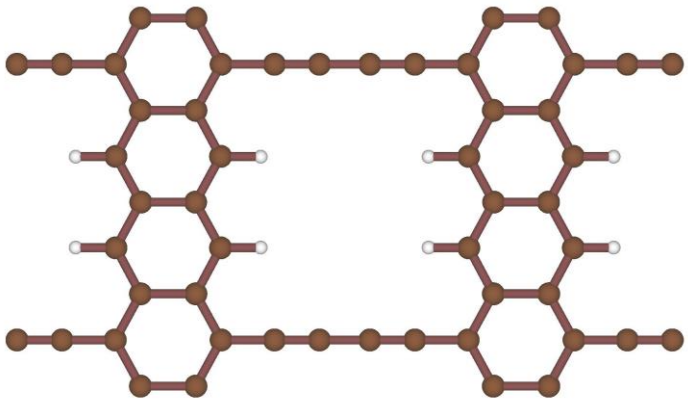

Figure 3: Top view of [1],[2]{2}-grazyne. The white spheres correspond to H atoms; the rest of atoms follow the colour-coding as on Figure 1.

5.4. Periodic unit cells

A crystalline solid is a solid material with a highly ordered atomistic structure, forming a crystal lattice that extends in all directions of space. The periodicity of the crystal structure is characterized by its primitive unit cell. The smallest group of particles in the material and their arrangement constitute the repeating pattern in the crystal. All the unit cells can be constructed from the primitive cell, but there is only one primitive cell, which is irreducible. Naturally, this structure contains the symmetry and structure of all the crystal in the three dimensions of space. The periodic pattern, also known as the Bravais lattice, is defined by three unit cell vectors (*a,b,c*) and three angles (*α, β, γ*), see Figure 4.

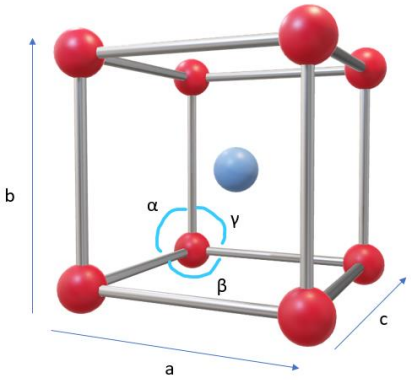

Figure 4: Unit cell of a bcc structure, red and blue spheres represent the atoms.

5.4.1. Reciprocal space

To study structures like grazynes, it is important to highlight the concept of reciprocal space, fundamental on describing the electronic behavior of electrons in the grazyne structure. This space arises from the need to solve the DFT equations in periodic systems, as it simplifies the mathematical calculations of the electronic structure by reducing the equidistant points with symmetry reasons. According to Bloch's theorem,[21] when translational symmetry is applied to a periodic unit cell, the wave function that solves the Schrödinger equation must also be periodic. According to this, this function can be written as the product of two components: A periodic function that reflects the symmetry of the lattice, and a planewave. This sum of planewaves is not described in real space, but in an abstract space called reciprocal space.

Reciprocal space is defined as the Fourier transform of real space.[22] So, while real space describes the position of the atoms in the crystal, reciprocal space describes how electronic waves propagate through that lattice behave. Mathematically, reciprocal space is defined by the vectors a*, b*, and c*, which are obtained from the real-space vectors a, b, and c using the following relationship:

$$a^* = 2\pi \frac{b \times c}{a \cdot (b \times c)} \; ; \; b^* = 2\pi \frac{c \times a}{b \cdot (c \times a)} \; ; \; c^* = 2\pi \frac{a \times b}{c \cdot (a \times b)} \quad (9).$$

These relationships show that reciprocal-space vectors are perpendicular to the planes defined by real-space vectors. Moreover, there is an inverse relationship between the two spaces: As the size of the unit cell increases in real space, the corresponding distances in reciprocal space decrease, and *vice versa*.

5.4.1.1. K-points

To carry out calculations in the reciprocal space without being computationally expensive, few **k**-points are used. These **k**-points represent discrete points in the reciprocal space where electronic properties are evaluated. The quality and accuracy of the calculations depend on how many **k**-points one used. One usually uses the Monkhorst-Pack method, which allows for the automatic generation of **k**-point meshes optimized for periodic systems for an automatic way, dividing the space in a mesh or grid of points, and evaluating bands at those nodes.

Furthermore, since the reciprocal space is defined by the periodicity of the system, when the crystal unit cell is larger in one direction, the size of the reciprocal space in that direction will be smaller, meaning that fewer **k**-points are needed to obtain accurate results at the bends dispersions in that direction. Conversely, in directions where the unit cell is small, a greater number of **k**-points are required to correctly represent the system dispersions.

5.5. Adsorption

To determine whether our material, the grazyne membrane, is an effective filter for separating molecules such as CO_2 and CH_4, it is necessary to study first how these molecules interact with the membrane. This interaction process is known as adsorption. It is important not to mix adsorption with absorption, as the first refers to a process in which molecules, or adsorbates, interact with the membrane or its surface. In contrast, absorption involves the molecules entering the membrane internal structure. There are two adsorption mechanisms depending on the interaction between the adsorbate and the surface: Chemisorption and physisorption. Chemisorption is a strong adsorption mechanism, in which atoms or molecules form true chemical bonds with the surface. This can lead to conformational changes or distortions of the adsorbed molecules and the material. This type of adsorption is selective and occurs specifically at active sites on the surface, whereas in the physisorption, the interaction with the surface is weaker and is usually due to van der Waals (*vdW*) dispersion forces, see Figure 5. Moreover, in this process, the adsorbates typically do not present structural changes, as they interact only weakly with the membrane.

To determine whether the adsorption of the studied molecules follows a chemisorption or physisorption mechanism, we can perform calculations and determine the adsorption energy, E_{ads}. This energy can be calculated as:

$$E_{ads} = E_{S/A} - E_S - E_A \quad (10),$$

where $E_{S/A}$ is the energy with the atom or molecule adsorbed on the material, E_S represents the material energy, and E_A is the energy of the adsorbate in vacuum. Within this definition a negative value of adsorption energy indicates a stabilization of the adsorbate over the surface, whereas a positive value indicates that both species are more stable separated than interacting. To ensure that the diffusion process occurs efficiently, it is desirable for the energy barrier to be below 1 eV. Given that this diffusion is characterized by low energy barriers, the interactions between the adsorbate and the membrane must be governed by physisorption forces, which yield small adsorption energies between 0 and -1 eV. When E_{ads} would be smaller than -1 eV, these materials would no longer be, *a priori*, suitable for use as filtering membranes, since molecules would stick to the membrane.

5.5.1. Penetration barriers

To study which of the halogenated substituted grazynes can act as a selective filter, allowing one of the two molecules, CO_2 or CH_4, to pass through it, is necessary to determine the penetration energy barrier. This energy can be calculated using the energy of the transition state, E_{TS}, and the energy of the molecules adsorbed on the surface, $E_{\mathrm{S/A}}$, according to the following expression:

$$E_b = E_{TS} - E_{S/A} \tag{11}.$$

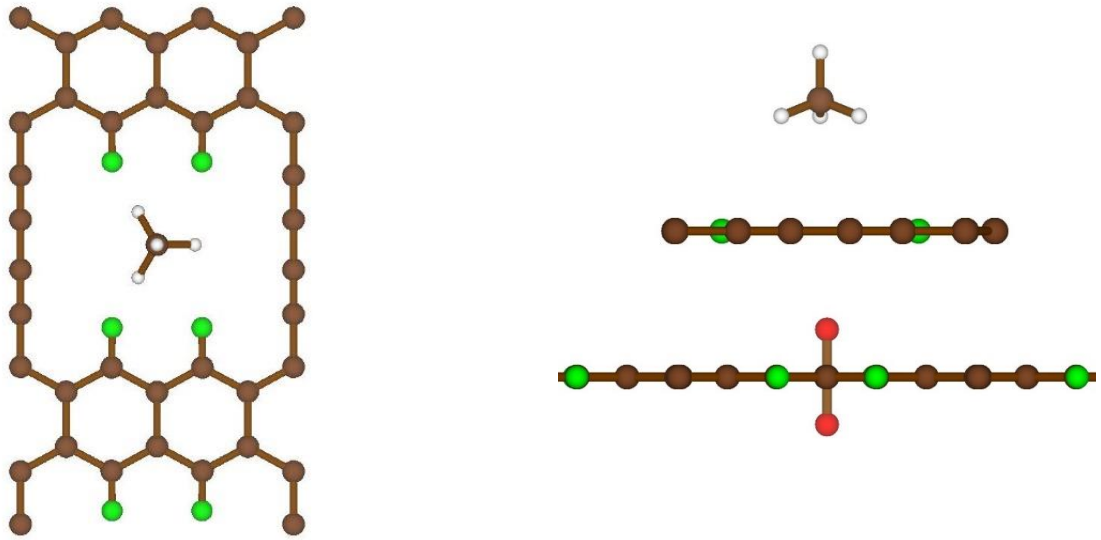

Figure 5: Top view of [1],[2],{2}-tetrafluorograzyne (left), and side views of the adsorbed methane (right top), and transition state of CO_2 diffusion (right bottom). Colour-code as in Figure 2, while red and green spheres denote Oxygen and Fluor atoms, respectively.

5.6. Diffusion rates

The rate at which a chemical reaction or process occurs can be described by the rate constant, *k*, which depends on both temperature *T*, and the process activation energy, E_a. This relationship is usually well described by the Arrhenius equation:

$$k = Ae^{-\frac{Ea}{RT}} \tag{12}.$$

In this equation, *A* is the pre-exponential factor, and *R* is the universal gas constant. Similar to Arrhenius equation, another possibility tis to obtain the rate constant from Transition State Theory (*TST)*, according to the following expression:

$$k = \frac{k_B T}{h} \cdot \frac{q^{\ddagger}}{q_r} e^{-\frac{\Delta \mathrm{E}^{\ddagger}}{k_B T}} \tag{13},$$

where, k_B is Boltzmann's constant, *h* is Planck's constant, $q^{\ddagger}$ refers to the partition function of the *TS*, and q_r correspond to the partition function of the reactant, in this context, the adsorbed molecule. $\Delta E^{\ddagger}$ represents the energy barriers required to reach the TS from the adsorbed state.

To calculate these partition functions correctly, it is important to understand that a molecule total partition function comes from different kinds of motions: Vibrations, rotations, translations, and electronic states. So, the overall partition function for a gas molecule is a product of the respective terms:

$$q = q_{vib} \cdot q_{rot} \cdot q_{trans} \cdot q_{elec} \tag{14}.$$

However, when a molecule is adsorbed on a surface, its rotational and translational movements are restricted due to interactions with the substrate and are actually converted into vibrations. As a result, only the vibrational partition function significantly contributes

to the calculation. In addition, because electronic transitions require large energy differences, their partition function is generally close to one, assuming that the molecule is in its ground electronic state.

Thus, one can calculate the vibrational contribution of the function as:

$$q_{vib} = \frac{1}{1-e^{-\frac{hv}{k_B T}}} \quad (15),$$

where vibrational frequencies, v_i, are estimated by DFT using finite displacement methods. For a molecule like CH_4, there are 3*N*-6 normal vibration modes, and for the CO_2 molecule, being a linear molecule, 3*N*-5 normal vibration modes, where *N* is the number of atoms. Note that a minimum has all real (non-imaginary) frequencies, while TS has one imaginary frequency.

Both E_{ads} and E_b terms have been corrected by applying the Zero-Point Energy (*ZPE*) correction, adding the E_{ZPE} according to,

$$E_{ZPE} = \frac{1}{2} \sum_i^{NMV} hv_i \quad (16),$$

where *h* is the Planck constant, and v_i each of the *NMV*. Note that the transition state imaginary frequency is not considered in the ZPE correction.

In the context of membranes, this imaginary vibrational frequency usually represents the associated movement for a molecule going through the membrane, from one side to the another. By studying this vibrational behaviour, we can better understand how different gases diffuse. For instance, the ability of CO_2 to pass through a membrane more easily than CH_4 can be estimated studying the selectivity of these two molecules. The selectivity can be defined as:

$$S_{CO_2/CH_4} = \frac{K_{CO_2}}{K_{CH_4}} = \frac{e^{-\frac{\Delta E^{\ddagger}_{CO2}}{k_B T}}}{e^{-\frac{\Delta E^{\ddagger}_{CH4}}{k_B T}}} \quad (17).$$

This ratio quantifies which gas is more likely to cross the membrane barrier, a crucial consideration in designing selective separation materials.

5.7. Molecular dynamics

MD is one of the most important methods for the determination of dynamic properties of chemical systems. The reliability of MD simulations is closely linked to the precision of the computational methods employed; however, achieving greater accuracy typically entails a higher computational cost. A very accurate method is AIMD,[23] where the interactions of atoms and electrons are calculated fully quantum mechanically from *ab initio* calculations, for example DFT calculations. Unfortunately, this method is limited to few atoms and small simulation times. An effective method of reducing the computational cost and accelerating these calculations is by using Force Fields (*FF*), which are parametrizations of the potential energy.

These parametrizations can range from very simple functions with only empirical parameters, to very complex functions parametrized using thousands of *ab initio* calculations. Developing high-quality FFs by hand is often a slow and demanding process. For this reason, in this project we will employ the ML-FF approach to accelerate this process; briefly explained next.

5.7.1. Machine learning force fields

In recent years, ML-FF have emerged as a great alternative to traditional methods for generating potential energy models in MD.[24] Here, in the prediction of the target property, the method automatically interpolates between known training systems that were previously calculated at *ab initio* level. The generation of FFs following this procedure is simpler than classical force fields generation because of taking advantage of the ML algorithm. During the run of the MD calculation, *ab initio* data is picked out and added to the training data. From the existing data, an FF is continuously built up. At each step of the simulation, the algorithm evaluates whether the current model is accurate enough. If not, a new *ab initio* calculation is performed, and the result is added to the training dataset. Over time, the FF becomes more reliable and reducing the number of DFT calculations needed, while slowly and steady turning the calculations towards ML-FF.

This process is guided by a probabilistic error model, named Bayesian error, which estimates how uncertain the FF predictions are. When confidence is high, the model skips additional calculations; when uncertainty is high, new data is acquired. As a result, the method balances accuracy and efficiency in a dynamic form, see Figure 6.

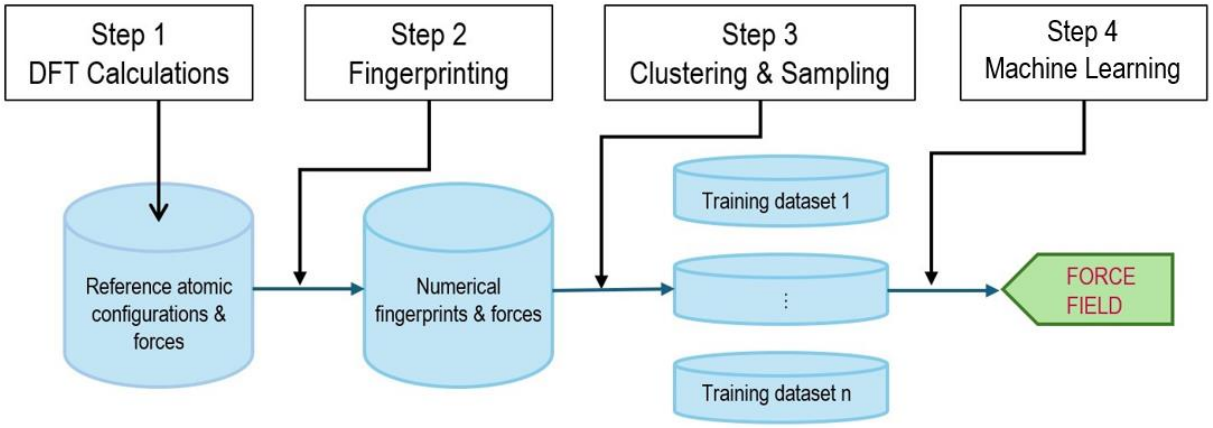

Figure 6: Workflow of the FF creation process using ML

6. COMPUTATIONAL DETAILS

All DFT calculations were done using VASP program suite.[18] The Projector Augmented Wave (*PAW*) method was used to describe core electrons,[25] while valence electrons were calculated using a planewave basis set of 415 eV, optimal in the description of grazynes and molecules upon. The exchange correlation effects were represented using the Perdew-Burke-Ernezerhof (*PBE*) exchange-correlation functional method,[26] in combination with Grimme's D3 dispersion forces description (PBE-D3).[27]

Isolated CO_2 and CH_4 geometries were fully optimized at **Γ k-**point in a cubic unit cell of 9×10×11 $Å^3$ dimensions. The electronic convergence threshold was set to 10^{-6} eV while the ionic convergence threshold was set to 10^{-5} eV. The structure of the [1],[1]-grazyne was initially considered and subsequently modified to introduce a defect in its crystalline lattice. This involved the removal of certain acetylenic bonds within the structure, leading to the formation of a pore. To stabilize the system, the dangling bonds around the pore were initially saturated with four hydrogen atoms. In this project, these hydrogen (H) atoms were progressively substituted by different halogens (F, Cl, and Br).

A vacuum of 10 Å was added perpendicularly to the membrane in *z* direction to prevent any interaction between the repeated membranes. This level of calculation reported energies converted below the chemical accuracy of 1 $kcal \cdot mol^{-1}$, *ca*. 0.04 eV. To perform the calculations of penetration barriers and adsorption energies, a carbon atom far from the defect site was fixed to avoid material drifting. Additionally, the carbon atoms of the studied molecules were constrained along the *z*-axis to maintain their orientation during the simulations. The frequency calculations were carried cut by finite displacements of 0.03 Å, constructing and diagonalizing the Hessian matrix.

All ML-FF MD simulations were performed in the NVT ensemble at 300 K, using a Norse-Hoover thermostat. A timestep of 1 fs was employed for a total of 50 ps simulation time. The simulation box included two molecules of CO_2 and CH_4 above the grazyne membrane in a vacuum slab, with periodic boundary conditions applied in the *x* and *y* directions.

7. RESULTS AND DISCUSSION

7.1. Study plan

With the aim of finding new structures capable of filtering biogas to achieves greater purity, this project aimed of studying various structures. The starting point has always been the structure shown in Figure 2, where the pore is saturated with hydrogen atoms. As can be seen in Figure 2, there are four atomic positions within the pore, where one, two, three, or even all four hydrogen atoms can be substituted. To continue the study, we studied possible substitution and used the following nomenclature: When the grazyne pore is substituted with a single fluorine atom and the remaining atoms are still hydrogen, the structure is referred to as [1],[2]{2}-fluorograzyne, see Figure 7. When two fluorine atoms are substituted, there are three possible structures: [1],[2]{2}-o-difluorograzyne (orto), [1],[2]{2}-p-difluorograzyne (para), and [1],[2]{2}-m-difluorograzyne (meta), see Figure 7.

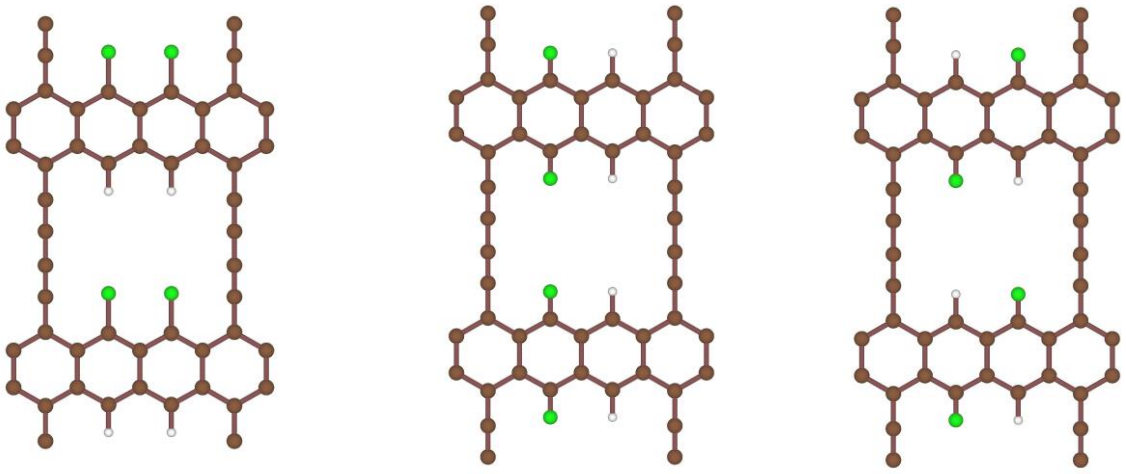

Figure 7: Top view of [1],[2]{2}-o-difluorograzyne (left), [1],[2]{2}-p-difluorograzyne structure (middle), and [1],[2]{2}-m-difluorograzyne (right). Colour-code as in Figure 2. Halogen atoms are shown as green spheres.

Similarly, when the structure contains three fluorine atoms, it is referred to as [1],[2]{2}-trifluorograzyne, and with four fluorine atoms, as [1],[2]{2}-tetrafluorograzyne. The same naming pattern is used for the structures containing chlorine and bromine atoms, which have also been studied in this project, but changing the name accordingly. Regarding the molecules studied, to carry out the diffusion and penetration barrier analysis, both CO_2 and CH_4 molecules were oriented perpendicularly to the grazyne membranes pore.

7.2. Diffusion process

The study of CO_2 diffusion through the different analysed membranes was carried out by DFT, first absorbing the molecule and getting de E_{ads}, and analysing the diffusion through the pore, and getting the penetration barrier energies E_b. For this purpose, the CO_2 molecule was initially placed 10 Å away from the center of the pore and then gradually moved toward the membrane in steps of 1 Å. During optimisations, the C atom of CO_2 and one C atom of the grazyne for away from the pore were kept fixed, allowing the molecule to rotate naturally along the reaction path while preventing any material drifting, and the same was done for CH_4.

7.2.1. Fluorine membranes

As previously mentioned, the CO_2 molecule was gradually approached to the membrane pore, until it was positioned entirely in the middle of the pore. At each step, a DFT calculation was performed to determine the energy of the system. It was observed that the CO_2 molecule became adsorbed at approximately 3 Å from the membrane, and the TS occurred when the molecule was located precisely within the membrane, at around 0.01 Å in height. Once the energies of the adsorbed state and the TS were obtained, the adsorption energies and penetration barrier energies were calculated and reported in Table 1. To simplify, notation is used as FG, o-2FG, p-2FG, m-2GF, 3FG and 4FG.

Grazyne	E_{ads} /eV	E_b /eV
FG	-013	0.15
o-2FG	-0.11	0.11
p-2FG	-0.10	0.26
m-2FG	-0.10	0.23
3FG	-0.08	0.46
4FG	-0.31	0.57

Table 1: E_{ads} and E_b values for CO_2 diffusion in fluorinated grazynes.

For an optimal diffusion process, the E_b values should be low. Additionally, it is desirable for the E_{ads} to be relatively low, as this would indicate a physisorption phenomenon, which is the type of interaction interests in for the membranes; they should not be sweeper materials. The values shown in Table 1 confirm that F-grazynes are structures capable of filtering CO_2. This is because, as observed, the structures exhibit small energy barrier below 1 eV, and adsorption energy values smaller than -0.35 eV.

The same procedure was carried out for methane. The CH_4 molecule was placed initially at the same position of CO_2, perpendicular to the centre of the pore and at a distance of 10 Å. The same parameters were calculated for CH_4, and the results are presented in Table 2.

Grazyne	E_{ads} /eV	E_b /eV
FG	-0.13	0.78
o-2FG	-0.15	1.19
p-2FG	-0.12	1.29
m-2FG	-0.11	1.33
3FG	-0.12	1.91
4FG	-0.36	2.37

Table 2: E_{ads} and E_b values for CH_4 diffusion in F-grazynes.

We can observe that, for the CH_4 molecule, the E_{ads} are of the same order of magnitude as those for the CO_2 molecule. This indicates that the interaction between methane and the membrane corresponds to a physisorption process and competitive and very weak, see Figure 8. However, when examining the E_b values associated to the diffusion process, we see a notable difference. In this case, most of the E_b values are above 1 eV, much higher than for CO_2, which would prevent CH_4 diffusion through the membrane.

Indeed, apart from the [1],[2]{2}-fluorograzyne structure, the F-grazynes would not allow methane diffusion across the membrane due to the high E_b values, see Figure 8. We can conclude that F-grazynes may be good candidates for biogas upgrading, as they enable the selective passage of CO_2 while preventing CH_4 from crossing, thus allowing for the separation of the two molecules.

Figure 8: Side view of TS (left) and adsorption state (right) of CH_4 in [1],[2]{2}-tetrafluorograzyne. Colour-code as in Figure 5.

7.2.2. Chlorine membranes

When studying chlorine grazynes, it is worth noting that the substitution with a heavier halide atom derive in a decrease of the pore size. The diffusion of CO_2 through the membrane lead to significantly enhanced E_{ads} and E_b, see Table 3.

Grazyne	E_{ads} /eV	E_b /eV
ClG	-0.16	1.35
o-2ClG	-0.34	1.96
p-2ClG	-1.12	3.40
m-2ClG	-0.97	3.48
3ClG	-0.72	4.28
4ClG	-1.71	5.04

Table 3: E_{ads} and E_b values for CO_2 diffusion in Cl-grazynes.

This increase indicate that the CO_2 molecule will stick to the grazyne, see figure 9, particularly for two to four Cl substitutions, except for o-2ClG case, and to a higher E_b, ranging from 1.35 to 5.04 eV, which will imply that CO_2 will hardly be able to permeate the membrane. This effect arises because chlorine atoms have a larger atomic radius, which effectively reduces the pore size increasing the barrier, and more polarizable electron densities, which can interact with CO_2, see Figure 9.

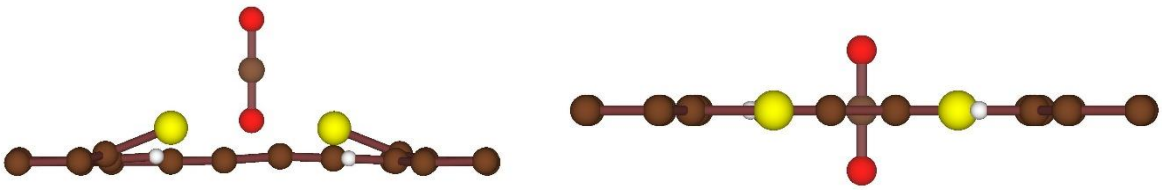

Figure 9: Side view of TS (left) and adsorbate state (right) of CO_2 in [1],[2]{2}-m-dichlorograzyne. Colour-code as in Figure 5, while yellow spheres denote Chlorine atoms.

For CH_4, see Table 4, the situation is similar. As the number of Cl atoms in the structure increases, the energy barriers also rise. This makes the CH_4 molecule even less able to penetrate the membrane, as it encounters a more significant energy barrier. CH_4, being a larger molecule compared to CO_2, faces a greater difficulty passing through the membranes pore, which in turn becomes smaller due to the larger atomic radius of Cl compared to F. Aside, except for ClG and o-2ClG, the E_{ads} are too large, implying CH_4 capture.

Grazyne	E_{ads} /eV	E_b /eV
ClG	-0.10	2.62
o-2ClG	-0.36	3.67
p-2ClG	-1.13	6.39
m-2ClG	-0.99	6.45
3ClG	-0.73	7.91
4ClG	-1.72	9.42

Table 4: E_{ads} and E_b values for CH_4 diffusion in Cl-grazynes.

From this one can conclude that chlorinated grazyne membranes would not be effective filters for biogas upgrading, since they essentially capture CO_2 and CH_4, and are non-permeable to them.

7.2.3. Bromine membranes

Finally, bromine substitutions are studied. The structures were kept unchanged; only the atoms surrounding the grazynes pore were replaced. As can be seen in Table 5, and visible in Figure 10, the overall behaviour is similar to the Cl case; the energy barriers are too high because of the size of Br. Therefore, the grazyne would be a capturing material, and non-permeable. Thus, halide substitutions for biogas upgrading are not viable except when F is used.

Grazyne	CO_2		CH_4	
	E_{asd} /eV	E_b /eV	E_{asd} /eV	E_b /eV
BrG	-0.81	2.38	-0.83	4.40
o-2BrG	-0.58	3.27	-0.58	5.30
p-2BrG	-1.95	5.50	-1.98	8.15
m-2BrG	-1.28	5.59	-1.32	9.30
3BrG	-1.01	7.03	-1.02	10.93
4BrG	-1.46	7.95	-1.47	12.86

Table 5: E_{ads} and E_b values for CO_2 and CH_4 diffusion in Br-grazynes.

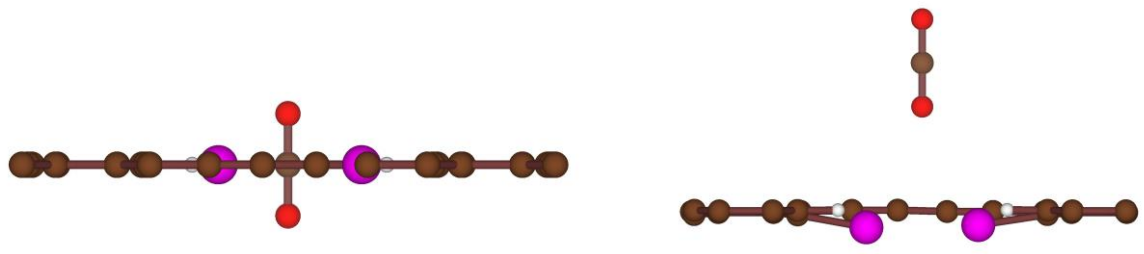

Figure 10: Side view of TS (left) and adsorption state (right) of CO_2 in [1],[2]{2}-o-Br-grazyne. Colour-code as in Figure 5.

7.3. Diffusion rates

After completing a thorough study on the diffusion of CO_2 and CH_4 through different halogen-substituted grazyne membranes, one can compute the rate constants for each molecule diffusion. The rates were calculated by using Eq. (15), and applying the ZPE, and shown in Figure 11 as a function of temperature. To carry out this study, a total of five different structures were selected: [1],[2]{2}-tetrafluorograzyne, [1],[2]{2}-trichlorograzyne, [1],[2]{2}-tetrachlorograzyne, [1],[2]{2}-o-dibromograzyne, and [1],[2]{2}-tetrabromograzyne. These structures were chosen because upon the completion of the study and deadline, were the ones able to accurate vibrational frequency values, essential for the rate constant calculations plus, they are a variety of representative structures.

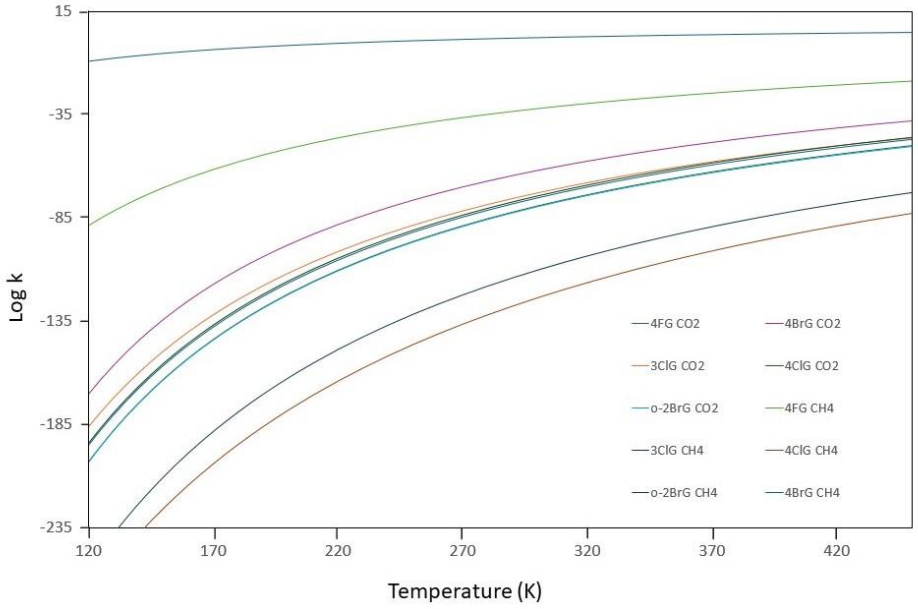

Figure 11: Variation of the rate constant logarithm with temperature for the studied structures

The temperature-dependent profiles of the logarithm of the rate constant k shown in Figure 11 revealed that only one structure exhibits positive values for log k, indicating that it would be the only structure that allow CO_2 molecules to pass through from the ones explored. This structure is [1],[2]{2}-tetrafluorograzyne, which, as previously confirmed by DFT calculations, shows optimal adsorption energies and diffusion penetration barriers for the selective filtration of CO_2 over CH_4, see Tables 1 and 2.

This result is further supported by the calculated diffusion rate constants. In the case of methane, although the values of log k remain negative across the entire temperature range for this structure, they are significantly lower compared to those of the other structures. This indicates that fluorinated grazynes are the only ones capable of selectively filtering biogas, enabling its upgrading by allowing the diffusion of CO_2 through the membrane while retaining CH_4. All other studied structures exhibit rate constant values close to zero, which suggests that none of them permit gas diffusion through the membrane in significant quantities. Substitution of H by Cl, or Br, just leads to CO_2 and CH_4 capable and non-permeability.

7.3.1. Selectivity

As indicated in Eq. (17), it is possible to calculate the diffusion selectivity of CO_2 through the grazyne membranes relative to CH_4, using the obtained rate constants. Among all the structures analyzed, only [1],[2]{2}-tetrafluorograzyne allows the passage of CO_2, being mostly impermeable to CH_4. This makes it the only structure relevant for evaluating the selectivity. This is shown in Figure 12, where the variation of the CO_2 selectivity over CH_4 as a function of temperature is represented. As observed, the selectivity is high at low temperatures, reaching values above 100, and gradually decreases as the temperature increases. This behavior can be explained by the fact that the thermal increase reduces the relative difference between the diffusion rates of both molecules, thereby lowering the effective selectivity of the membrane. Aside, the enrichment at 300 K with a selectivity of 38 would imply that in a CO_2/CH_4 mix of equal parts, the stream could be enriched up to 80%, opening the path towards purities above 95% by few membrane cycles.

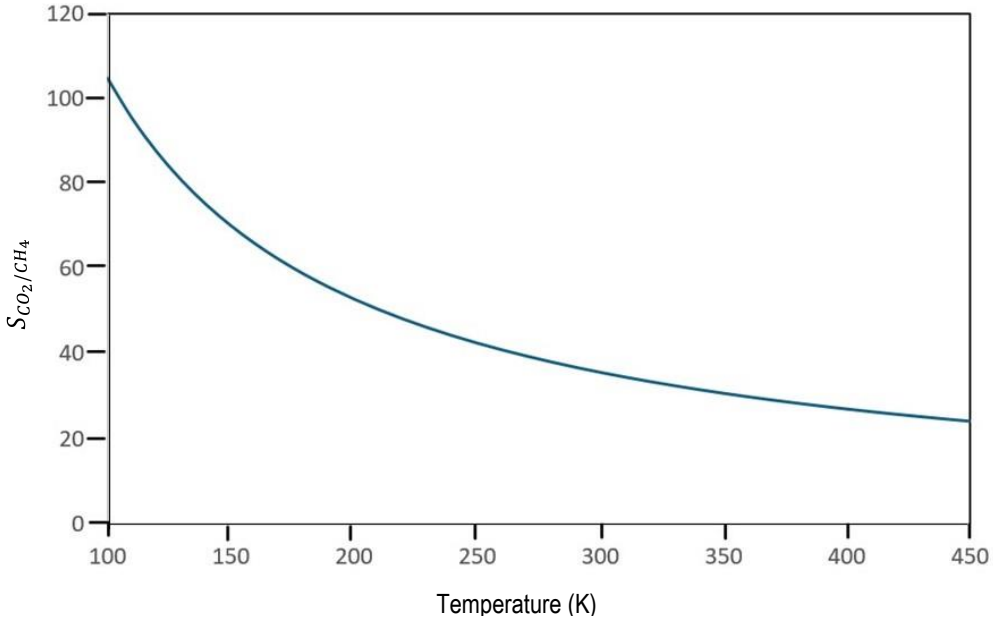

Figure 12: Variation of CO_2 selectivity over CH_4 with temperature for the [1],[2]{2}-tetrafluorograzyne structure.

Overall, these results indicate that [1],[2]{2}-tetrafluorograzyne could functions as a highly selective filter for CO_2 over CH_4, particularly under low-temperature conditions, where the selectivity reaches its most significant values.

7.4. Molecular dynamics with ML-FF method

In order to assess the stability and reliability of the halogenated grazyne membranes beyond static DFT calculations, MD were performed by employing ML-FF. These simulations were used to analyze the time evolution of the system, considering both thermodynamics and kinetics aspects of gas separation. The ML-FF generation workflow in VASP consist of three main steps: train, refit, and run. In the train step, atomic configurations were generated along with their DFT energies and forces. These were employed to develop the initial version of the FF, see Figure 6. Then, when the FF is enough trained, a refit is performed. The FF was improved by adding new configurations, especially those where the model was uncertain (based on the Bayesian error). Finally, in the run step the trained FF was used to run MD simulations at 300 K under NVT conditions, with 50,000 timesteps of fs, 50 ps in total. These simulations aimed to model how CO_2 and CH_4 molecules interact with the [1],[2]{2}-FG and [1],[2]{2}-o-2FG membranes over time.

The training seemed to work well at first; the ML-FF diagnostics showed good agreement between predicted and DFT forces and energies, with low error values, see Figure 13, containing the Root Mean Square Error (*RMSE*). The energy errors are below 0.5 meV per atom, and on Forces of 56 meV/ Å.

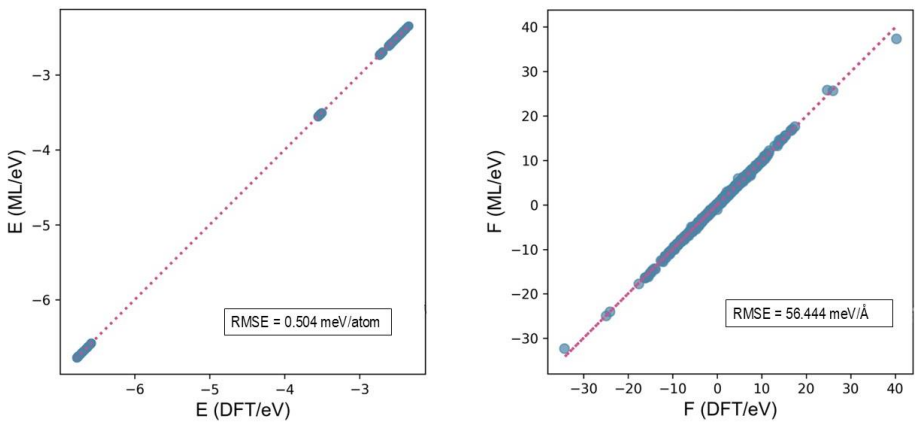

Figure 13: Parity plot of energies (left) and forces (right), and corresponding RMSE.

Still, during the run simulations, strange and unrealistic molecular behaviours were seen. For example, CO_2 molecules appeared bent instead of linear, and other unnatural distortions occurred, with the results not being chemically correct, see Figure 14.

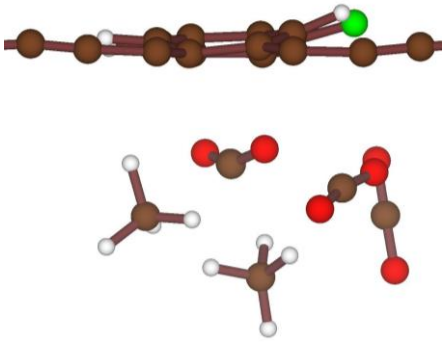

Figure 14: Snapshot of a CO_2 and CH_4 mixture over FG model under ML-FF MD. Colour code as in Figure 5.

To understand the origin of these chemically unrealistic distortions observed during the MD run a detailed analysis of the simulation outputs was conducted. Figure 15 shows the time evolution of key thermodynamic properties: temperature, free energy, and potential energy. These plots were evaluated over the entire 50 ps MD trajectory.

From the temperature graph, a sharp spike is observed around time step 12.5 ps where the system temperature increases dramatically. Simultaneously, the corresponding free energy and potential energy plots also show significant abrupt changes at the same time step. This sudden deviation strongly indicates that a structural anomaly occurred during the run.

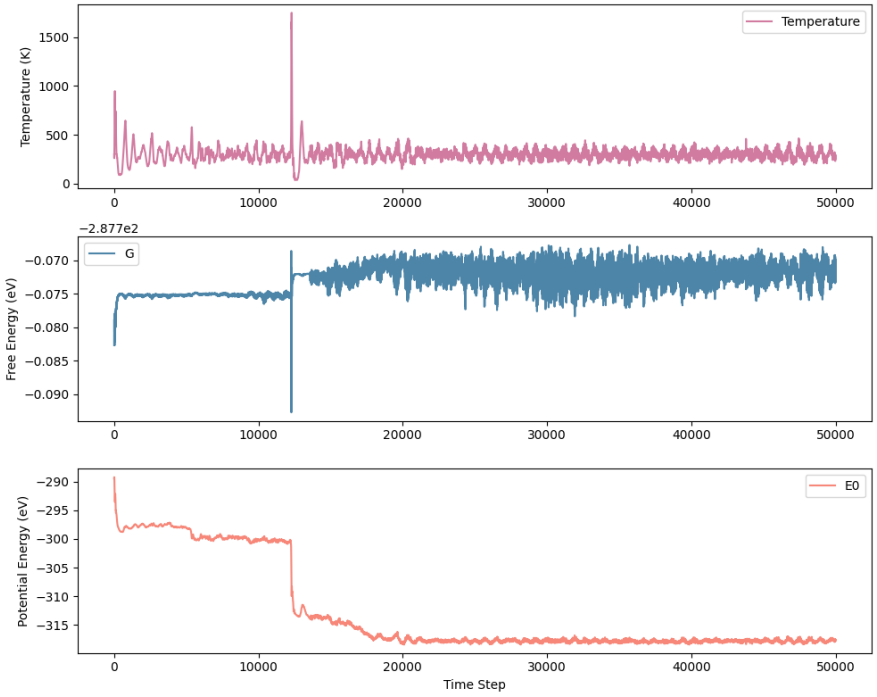

Figure 15: The time evolution of temperature (top), free energy (middle), and potential energy (bottom) during ML-FF run.

This suggests that the ML-FF was not well trained. The training data may not have covered enough situations or explored the full space of configurations needed. At that moment, the ML-FF likely encountered an atomic configuration outside the scope of its training data, leading to poor force predictions and thus causing the system to evolve toward non-physical geometries, *e.g.* bent CO_2. Because of this, the force field was not reliable enough to simulate the real chemical behaviour of the system, aslep that is left for future research.

In short, ML-FF is a powerful method for running faster simulations on bigger systems, but in this case, the force field was not accurate enough. Due to limited project time, the training process could not be fully completed. Future work should include a much longer and more detailed training phase to build a force field that can correctly simulate CO_2 and CH_4 dynamics in halogenated grazynes.

8. CONCLUSIONS

Based on the results obtained throughout this work, the following conclusions can be listed:

- In fluorinated grazynes, CO_2 shows low adsorption energies and low diffusion barriers, while CH_4 also shows low adsorption energies but high diffusion barriers. Both molecules interact *via* physisorption, but only CO_2 can diffuse through the membrane. This makes fluorograzynes good candidates for biogas upgrading, allowing CO_2 to pass while retaining CH_4.
- Chlorinated and brominated grazynes strongly adsorb both gases, leading to chemisorption processes and blocking their diffusion. This makes them unsuitable for gas separation
- Only tetrafluorograzyne showed positive diffusion rates for CO_2 and high CO_2/CH_4 selectivity at low temperatures, feasible for biogas upgrading.
- ML-FF training showed low errors, but MD runs produced unphysical results, *e.g.* bent CO_2, indicating that the force field are not yet reliable, and more training and fitting is necessary to run the MD simulations.

9. REFERENCES AND NOTES

1. Feichter, J.; Seifert, U.; Zellner, R. Luftchemie und Klima. Chem. Unserer Zeit, **2007**, 41, 138–150.
2. Wu, L.; Wei, W.; Song, L.; Wozniak-Karczewska, M.; Chrzanowski, L.; Ni, B.-J. Upgrading biogas produced in anaerobic digestion: biological removal and bioconversion of CO_2 in biogas. Renew. Sustain. Energy Rev., **2021**, 150, 111448.
3. Sun, Q.; Li, H.; Yan, J.; Liu, L.; Yu, Z.; Yu, X. Selection of appropriate biogas upgrading technology, a review of biogas cleaning, upgrading and utilisation. Renew. Sustain. Energy Rev., **2015**, 51, 521–532.
4. Del Rosario, M.; Munoz, R.; Gonzalez-Sanchez, A.; Ruiz, A.; Quijano, G. Membrane materials for biogas purification and upgrading fundamentals, recent advances and challenges. J. Environ. Chem. Eng., **2024**, 12, 114106.
5. Kunkel, C.; Viñes, F.; Illas, F. Biogas Upgrading by transition metal carbides. ACS Appl. Energy Mater., **2018**, 1, 43-47.
6. Prats, H.; Mcaloone, H.; Viñes, F.; Illas, F. Ultra-high selectivity biogas upgrading through porous MXenes. J. Mater. Chem. A, **2020**, 8, 12296–12300.
7. Chen, J. J.; Li, W. W.; Li, X. L.; Yu, H. Q. Improving biogas separation and methane storage with multilayer graphene nanostructure via layer spacing optimization and lithium doping: a molecular simulation investigation. Environ. Sci. Technol., **2012**, 46, 10341–10348.
8. Covarrubias-García, I.; Quijano, G.; Aizpuru, A.; Sánchez-García, J. L.; Rodríguez-López, J. L.; Arriaga, S. Reduced graphene oxide decorated with magnetite nanoparticles enhance biomethane enrichment. J. Hazard. Mater., **2020**, 397, 122760.
9. Kang, J.; Wei, Z.; Li, J. Graphyne and its family: recent theoretical advances. ACS Appl. Mater. Interfaces, **2019**, 11, 2692–2706.
10. Du, N.; Park, H. B.; Dal-Cin, M. M.; Guiver, M. D. Advances in high permeability polymeric membrane materials for CO_2 separations. Energy Environ. Sci., **2012**, 5, 7306–7322.
11. Bara, J. E.; Camper, D. E.; Gin, D. L.; Noble, R. D. Room-temperature ionic liquids and composite materials: platform technologies for CO_2 capture. Acc. Chem. Res., **2010**, 43, 152–159.
12. Kosinov, N.; Gascon, J.; Kapteijn, F.; Hensen, E. J. M. Recent developments in zeolite membranes for gas separation. J. Membr. Sci., **2016**, 499, 65–79.
13. Kang, Z.; Fan, L.; Sun, D. Recent advances and challenges of metal–organic framework membranes for gas separation. J. Mater. Chem. A, **2017**, 5, 10073–10091.
14. Wang, M.; Zhao, J.; Wang, X.; Liu, A.; Gleason, K. K. Recent progress on submicron gas-selective polymeric membranes. J. Mater. Chem. A, **2017**, 5, 8860–8886.
15. Kamalinahad, S.; Viñes, F.; Gamallo, P. Grazynes: carbon-based two-dimensional composites with anisotropic properties. J. Phys. Chem. C, **2019**, 123, 27140–27149.
16. Viñes, F.; Calzada, A.; Gamallo, P. Thermodynamic, kinetic and dynamic aspects of biogas upgrading using nano-engineered grazynes. J. CO_2 Util., **2023**, 71, 102459.
17. Calzada, A.; Viñes, F.; Gamallo, P. On the CO_2 harvesting from N_2 using grazyne membranes. ChemSusChem, **2024**, 17, 852–870.
18. Kresse, G.; Furthmüller, J. Efficiency of ab-initio total energy calculations for metals and semiconductors using a plane-wave basis set. Comput. Mater. Sci., **1996**, 6, 15–50.
19. Kohn, W.; Sham, L. J. Self-consistent equations including exchange and correlation effects. Phys. Rev. A, **1965**, 120, 23698–23706.
20. Hohenberg, P.; Kohn, W. Inhomogeneous electron gas. Phys. Rev., **1964**, 136, 864.
21. Martínez-Duart, J. M.; Martín-Palma, R. J.; Agulló-Rueda, F. Survey of solid-state physics. In Nanotechnology for microelectronics and optoelectronics, **2006**, 21–53.
22. Shah, M.; Sung, S. H.; Hovden, R. The atlas of Fourier transforms: a guide to reciprocal space for biologists and materials scientists. Microsc. Microanal., **2024**, 30, 1–2.
23. Marx, D.; Hutter, J. Ab initio molecular dynamics: Theory and implementation. In *Modern methods and algorithms of quantum chemistry*, **2009**, 301–449.
24. Huan, T. D.; Batra, R.; Chapman, J. A universal strategy for the creation of machine learning-based atomistic force fields. NPJ Comput. Mater., **2017**, 3, 37.
25. Blöchl, P. E. Projector augmented-wave method. Phys. Rev. B, **1994**, 50, 17953–17979.
26. Perdew, J. P.; Burke, K.; Ernzerhof, M. Generalized gradient approximation made simple. Phys. Rev. Lett., **1996**, 77, 3865–3868.
27. Grimme, S.; Antony, J.; Ehrlich, S.; Krieg, H. A consistent and accurate ab initio parametrization of density functional dispersion correction (DFT-D) for the 94 elements H–Pu. J. Chem. Phys., **2010**, 132, 154104.

10. ACRONYMS

AIMD: *Ab Initio* Molecular Dynamics

BO: Born-Oppenheimer

BrG: Bromograzyne

CI: Configuration Interactions

ClG: Chlorograzyne

DFT: Density Functional Theory

FG: Fluorograzyne

GGA: Generalized Gradient Approximation

HF: Hartree-Fock

HK: Hohenberg-Kohn

KS: Kohn-Sham

LDA: Local Density Approximation

MD: Molecular Dynamics

ML-FF: Machine Learning Force Fields

MP: Møller-Plesset

PAW: Projector Augmented Wave

PBC: Periodic Boundary Conditions

PBE: Perdew-Burke-Ernzerhof

RMSE: Root Mean Square Error

TS: Transition State

VASP: Vienna *Ab initio* Simulation Package

xc: exchange-correlation

ZPE: Zero-Point Energy